FULafia Journal of Science & Technology
ISSN (print) 2449-0954 \ ISSN (online) 2636-4972
https://lafiascijournals.org.ng/index.php/fjst
Sponsored By TERTIARY EDUCATION TRUST FUND
Manuscript => Received: Feb., 2026; Accepted: May, 2026; Published: May, 2026 https://doi.org/10.62050/fjst2026.v10n2.817

AEROMAGNETIC SPECTRAL INVESTIGATION OF SUBSURFACE THERMAL STRUCTURE FOR GEOTHERMAL ENERGY EVALUATION IN YOLA ARM, UPPER BENUE TROUGH, NIGERIA

Lucky Peter Kenda[1,2]*, Adetola Sunday Oniku[2], Bello Yusuf Idi[2], Yohanna Andarawus[3] and Sebastian, Abraham Sunu[2,4]
[1]*Department of Physics, Taraba State University, Jalingo, Taraba State, Nigeria*
[2]*Physics Department, Modibbo Adama University, Yola, Adamawa State, Nigeria*
[3]*Department of Geology, Federal University of Lafia, Nasarawa State, Nigeria*
[4]*Department of Petroleum Chemistry & Physics, American University of Nigeria (AUN), Adamawa State*
*Corresponding email: kendalucky1@gmail.com

ABSTRACT
Geothermal resources are increasingly recognized as a reliable and sustainable energy option for Nigeria. Despite previous investigations, a detailed characterization of subsurface thermal conditions, particularly within structurally complex basins such as the Upper Benue Trough, is required. This research investigates the potential for geothermal energy in Yola Arm by using spectral analysis of high-resolution aeromagnetic data. Six aeromagnetic sheets from the Nigerian Geological Survey Agency were processed with Oasis Montaj 8.4. The Magnetic data were corrected for low-latitude effects through Reduction to the Magnetic Equator, followed by separation of regional and residual components to isolate shallow anomalies. The residual data were partitioned into 28 overlapping segments for spectral analysis. Radially averaged power spectrum analysis was applied to evaluate Curie point depth (CPD), geothermal gradient, and heat flow. The results indicate that CPD varies between approximately 14 km and 26 km. Corresponding geothermal gradients range from about 22 to 39 °C/km, while heat flow values fall within 56 mW/m² and approximately 100 mW/m². Zones characterized by relatively shallow CPD exhibit higher thermal gradients and enhanced heat flow, suggesting favourable geothermal conditions. Conversely, deeper CPD zones are associated with lower thermal regimes. Spatial distribution patterns indicate that the southeastern portion of the area under study possesses a potential for geothermal energy.

Keywords: Geothermal energy, Aeromagnetic data, Spectral analysis, Curie point depth, Heat flow.

INTRODUCTION
Geothermal energy has become a vital part of the world's shift to low-carbon and sustainable energy systems due to its reliability and independence from climatic variability (International Renewable Energy Agency, 2020). Unlike many sources of renewable energy, geothermal energy provides a reliable and continuous supply of power, independent of weather conditions, making it particularly suitable for base-load electricity generation. Its relatively low greenhouse gas emissions and long-term sustainability further enhance its attractiveness as an alternative energy resource (Ayuba & Lawal, 2019; Dickson & Fanelli, 2014; DiPippo & Renner, 2014). The occurrence and distribution of geothermal resources are largely controlled by subsurface thermal conditions, which are influenced by geological structures, tectonic settings, and lithological variations (Bhattacharyya & Leu, 1975; Ruban, 2015).
One of the most reliable parameters for assessing subsurface thermal structure is the Curie point depth (CPD), defined as the depth at which magnetic materials lose their ferromagnetic characteristics due to high temperatures, and it is usually approximately 580 °C (Blakely, 1996; Tanaka *et al*., 1999). CPD serves as an indirect indicator of geothermal gradient and heat flow, and has been widely used in geothermal investigations (Okubo *et al*., 1985). Aeromagnetic data provide an efficient and cost-effective means of estimating CPD and related thermal parameters (Okubo *et al*., 1985). Spectral analysis techniques, particularly radially averaged power spectrum methods, have proven effective in determining the depth to magnetic sources by analyzing the frequency characteristics of magnetic anomalies(Bhattacharyya & Leu, 1975; Spector & Grant, 1970).
The Upper Benue Trough is a major Cretaceous rift basin created when the African and South American continents split apart (Wright *et al*., 1985). It is characterized by complex structural features, including faults, folds, and igneous intrusions, which significantly influence its thermal regime (Benkhelil, 1989; Nur *et al*., 1999; Obande *et al*., 2014). Prior research in the Benue Trough reported variations in Curie depth and heat flow, suggesting localized geothermal potential (Abangwu *et al*., 2023; Anakwuba & Chinwuko, 2015; Nwankwo, 2015; Obande *et al*., 2014; Salako, 2014; Yakubu *et al*., 2023). In order to support current efforts in geothermal resource evaluation in Nigeria, this research focuses on the Yola Arm to assess its geothermal energy potential through spectrum analysis of high-resolution aeromagnetic data.

MATERIALS AND METHODS

Location and Geology of the Area under Study

The research region (Fig. 1) is located in northeastern Nigeria's Upper Benue Trough, between latitudes 9°00′00° and 10°00′00° N and longitudes 11°30′00° to 13°00′00° E, covering an area of approximately 18,481.5 km², and is geologically characterized by a complex assemblage of Precambrian Basement Complex rocks and Cretaceous sedimentary sequences (Fig. 2). The basement rocks are dominated by gneiss, migmatite, augen gneiss, granite gneiss, hornblende granite, and coarse to medium-grained granitic intrusions, which represent metamorphosed meta-sediments and older granites that have undergone intense deformation and magmatic reworking during Precambrian tectonothermal events, with the augen gneisses exhibiting distinctive eye-shaped feldspar porphyroclasts formed by deformation (Carter, 1963; Obaje, 2009; Rahaman, 1988; Wright *et al*., 1985). These crystalline basement rocks are unconformably overlain by Albian Cretaceous sedimentary units of the Benue Trough, including Bima Sandstone, Yolde Formation, and Dukul Formation, together with associated shale, limestone, and calcareous sandstone. Bima Sandstone, which forms the basal sedimentary unit of Benue Trough, rests directly on the basement complex, is largely derived from granitic source rocks, and is characterized by feldspathic lower beds that grade upward into less feldspathic sandstones (Carter, 1963; Kasidi, 2019; Zaborski *et al*., 1997). The lower parts of the sedimentary succession consist predominantly calcareous sandstone and shale, reflecting a transition from continental depositional environments to shallow marine conditions, with localized limestone beds near base marking Yolde Formation, while younger sedimentary units such as the Dukul Formation reflect continued marine influence (Obaje, 2009; Zaborski *et al*., 1997). Recent alluvial deposits occur along major drainage channels, consisting of unconsolidated sands, silts, and clays derived from the weathering of both basement and sedimentary rocks (Obaje, 2009; Nigerian Geological Survey Agency, 2006).

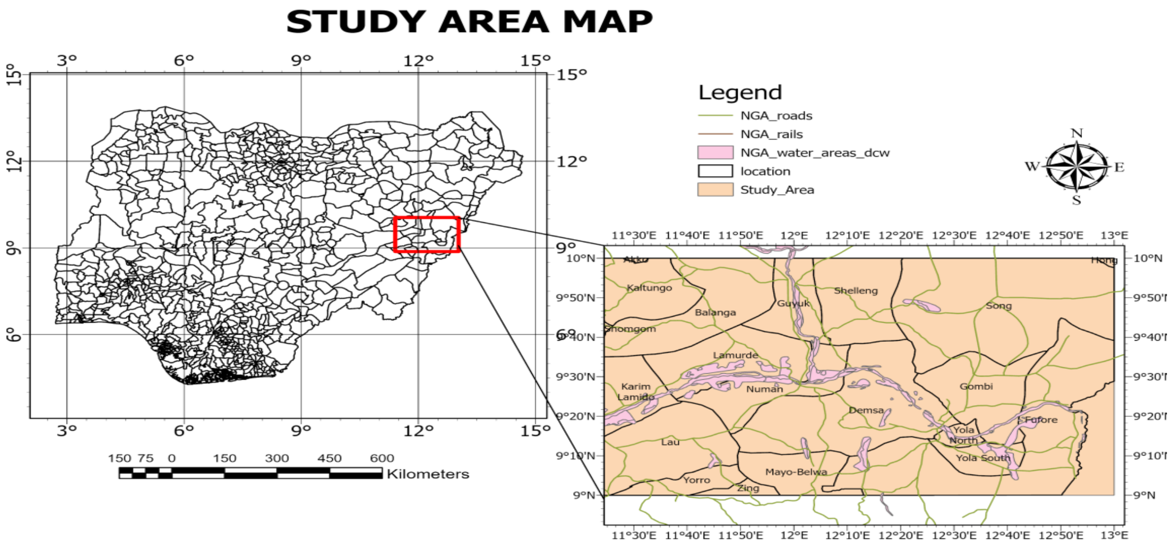

Figure 1: The research area map

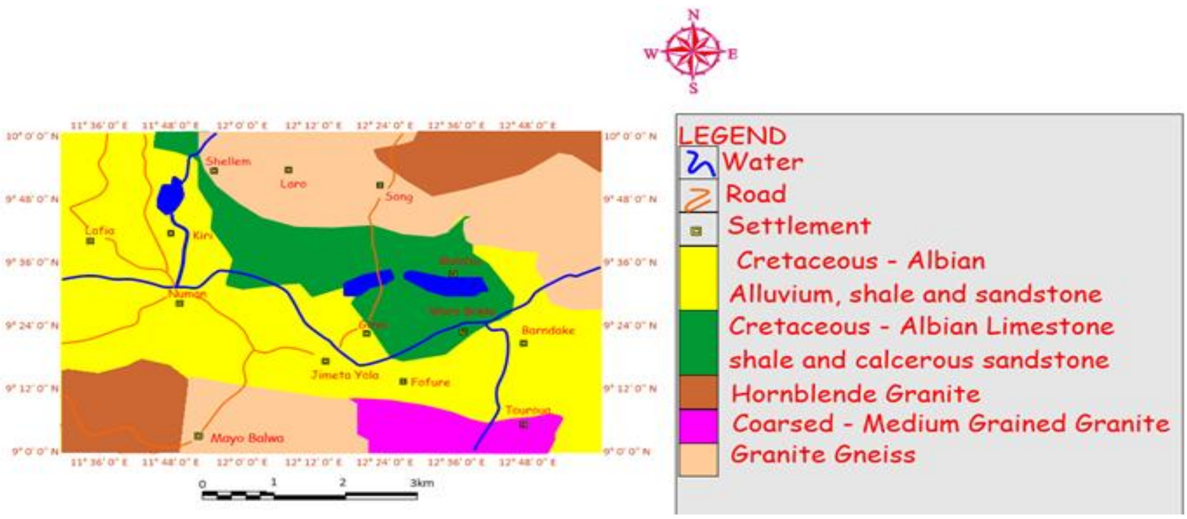

Figure 2: Geology map of the research area

Aeromagnetic Datasets

High-resolution aeromagnetic datasets covering six map sheets (Guyuk, Shellen, Zummo, Dong, Numan, and Gerei) were utilized in this study. The aeromagnetic datasets used were acquired from the Nigerian Geological Survey Agency and originally collected by Fugro Airborne Surveys Limited. These datasets typically have flight line spacing of 500 m and terrain clearance of approximately 80-100 m, ensuring high spatial resolution suitable for detailed subsurface investigations (Reeves, 2005). Initial data processing involved standard corrections, removal of the International Geomagnetic Reference Field (IGRF), levelling, and micro-levelling to eliminate line-based noise and ensure data consistency (Minty, 1997; Oladunjoye *et al*., 2016; Patterson & Reeves, 1985). Reduction to the Magnetic Equator (RTE) filter was used to appropriately position magnetic anomalies over their causal sources because the study location is located within a low magnetic latitude region (Blakely, 1996; Telford *et al*., 1990). The residual field was divided into overlapping spectral windows to minimize edge effects during analysis (Spector & Grant, 1970). The slopes of the logarithmic power spectrum were used to calculate the Curie point depth (Z_b).

$$Z_b = 2Z_0 - Z_t \qquad (1)$$

Following Tanaka *et al*. (1999), geothermal gradient (dT/dz) was estimated assuming a Curie temperature of 580 °C, while heat flow (Q) was derived using Fourier's law:

$$Q=\lambda\left(\frac{dT}{dz}\right)=\lambda\left(\frac{580\ °\mathrm{C}}{Z_b}\right) \qquad (2)$$

where λ represents thermal conductivity, typically assumed to be 2.5 W/m°C for crustal rocks (Ruban, 2015; Tanaka *et al*., 1999; Turcotte & Schubert, 2002).

RESULTS AND DISCUSSION

The Total Magnetic Intensity (TMI) map (Fig. 3) reveals significant spatial variations in magnetic values 31178.39 to 31355.91 nT, with higher intensities predominantly observed in the northern and southeastern parts of the research area. The anomalies are likely associated with magnetite-rich rocks, magmatic intrusions or volcanic units, which produce strong magnetic responses (Telford *et al*., 1990). In contrast, areas with lower magnetic values, particularly in the southern and northeastern zones, are interpreted as regions dominated by sedimentary formations or weakly magnetic materials (Reeves, 2005; Salako *et al*., 2019).

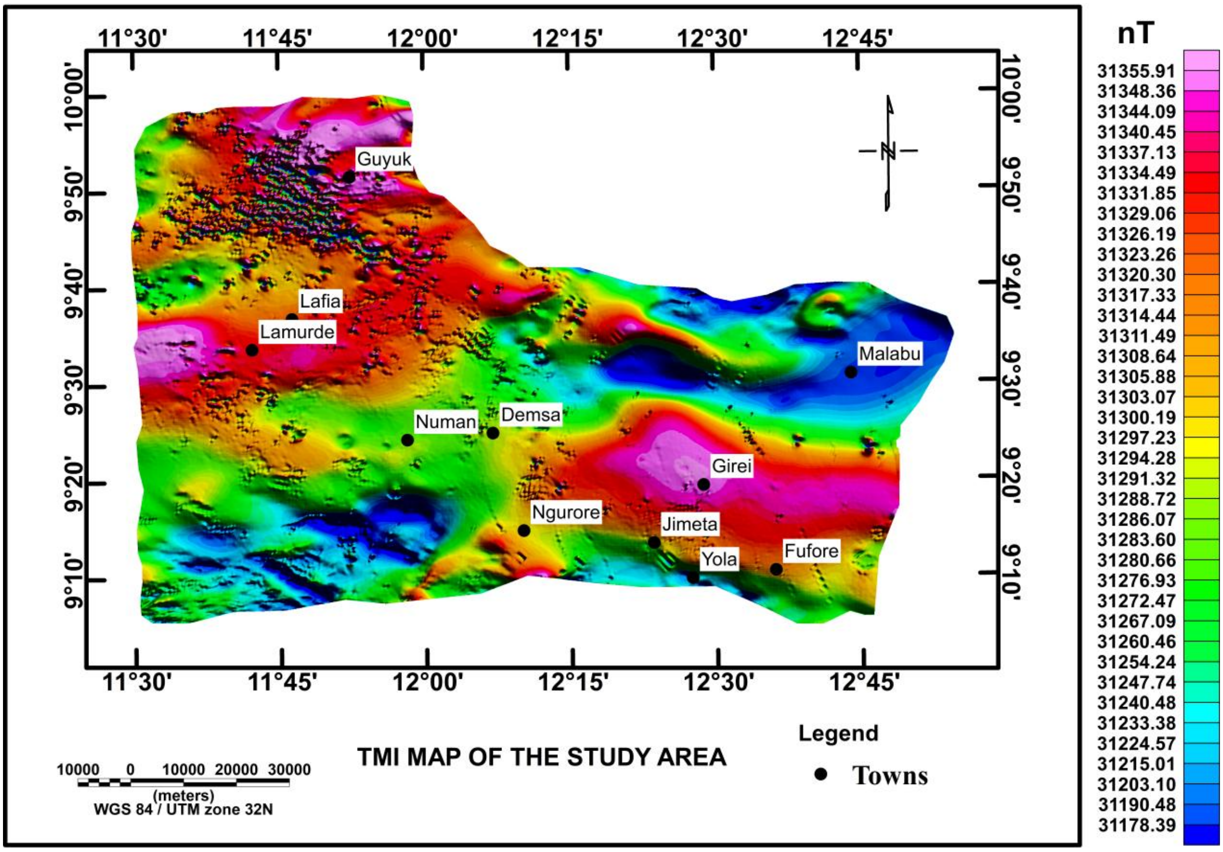

Figure 3: Map showing the area's total magnetic field intensity

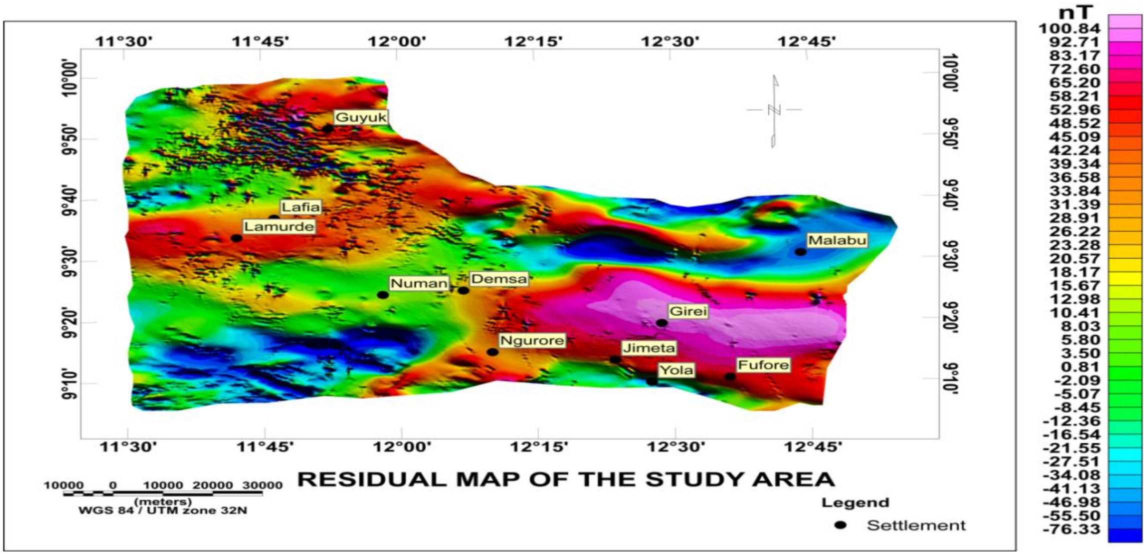

Figure 4: Map showing the research area's residual magnetic field intensity

The Residual Magnetic Intensity (RMI) map (Fig. 4) with magnetic anomalies ranging from -76.33 to 100.84 nT highlights shallow magnetic sources, with pronounced anomalies in the southeastern region of the area under study. These anomalies indicate variations in near-surface lithology and structural features. Regions exhibiting low residual values are interpreted as areas with deeper basement or less magnetic rock units (Blakely, 1996; Nabighian *et al*., 2005).

Residual magnetic analysis enhances shallow features and reveals structural trends consistent with regional tectonic patterns. The dominant NW-SE structural orientation aligns with known tectonic trends in the Benue Trough, which are associated with rifting and crustal deformation processes (Benkhelil, 1989). Such structural features, including faults and fractures, are important as they can act as conduits for geothermal fluid circulation (Anudu *et al*., 2014, 2020; Hochstein, 1990; Nabighian *et al*., 2005).

The residual magnetic intensity (RMI) data were subdivided into 28 overlapping square blocks (Fig. 5) to ensure continuous spatial coverage and to minimize edge-related artefacts during the analysis.

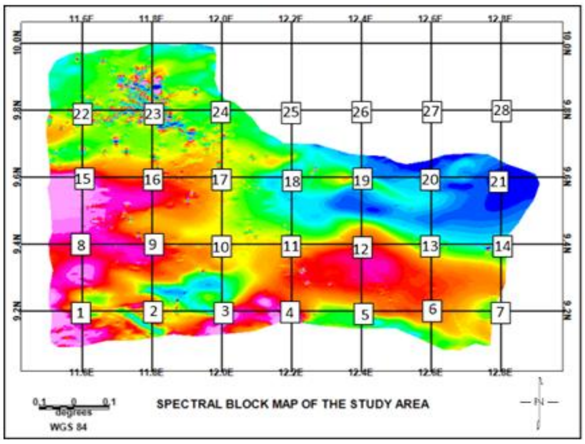

Figure 5: Residual magnetic field intensity showing blocks

For each segment, the Curie point depth (CPD), geothermal gradient, and heat flow were estimated using the radial power spectrum technique. For each block, spectral energy curves were created and shown as the natural logarithm of energy against frequency. Representative plots selected for blocks 1, 3, 13, 14, 23, and 24 are presented in Fig. 6. The calculated CPD, geothermal gradient, and heat flow values for all blocks are summarized in Table 1.

Spectral analysis results indicate that Curie point depths range between approximately 14 km and 26 km, with an average of about 21 km (Fig. 7). These values fall within the range reported for geothermal provinces and sedimentary basins worldwide (Nwankwo & Ekine, 2009; Tanaka *et al*., 1999). Shallow CPD values are indicative of elevated subsurface temperatures and possible magmatic influence, suggesting enhanced geothermal potential (Okubo *et al*., 1985).

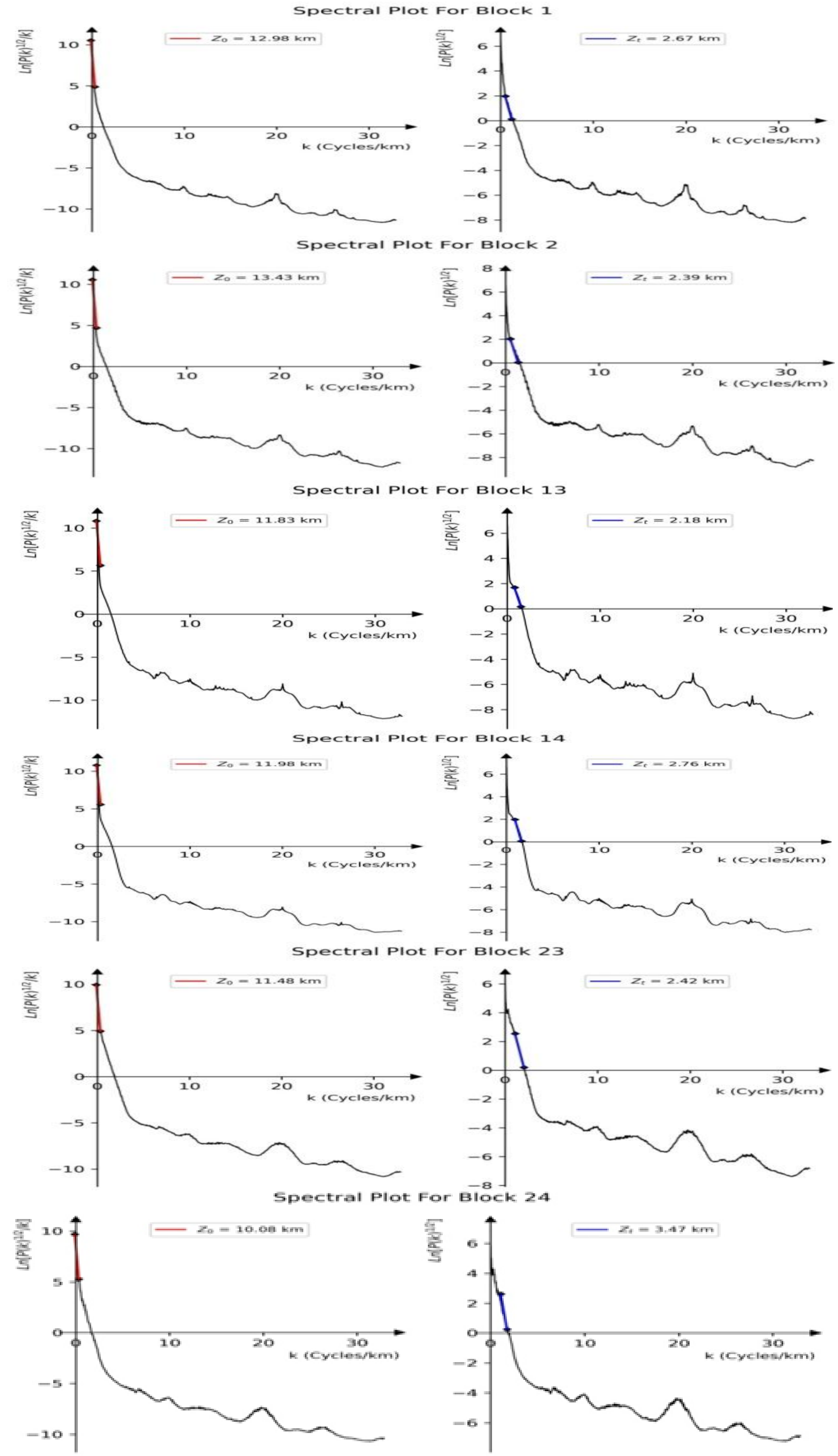

Figure 6: Logarithmic graphs of the spectral energy for block plots 1, 3, 13, 14, 23 and 24

Table 1: Estimated Curie point depth, geothermal gradient and heat flow of the research area from spectral analysis

S/N	Spectral Block	Longitude (°)	Latitude (°)	Z_0(Km)	Z_t(Km)	Z_b(Km)	$\frac{dT}{dZ}(CKm^{-1})$	$Q(mWm^{-2})$
1	Block 1	11.6	9.2	12.98	2.67	23.29	24.903	62.258
2	Block 2	11.8	9.2	13.43	2.39	24.47	23.702	59.256
3	Block 3	12	9.2	11.75	2.7	20.8	27.885	69.712
4	Block 4	12.2	9.2	11.78	2.2	21.36	27.154	67.884
5	Block 5	12.4	9.2	12.03	3.44	20.62	28.128	70.320
6	Block 6	12.6	9.2	8.62	2.28	14.96	38.770	96.925
7	Block 7	12.8	9.2	9.11	3.26	14.96	38.770	96.925
8	Block 8	11.6	9.4	13.42	2.03	24.81	23.378	58.444
9	Block 9	11.8	9.4	11.78	2.59	20.97	27.659	69.146
10	Block 10	12	9.4	12.22	2.56	21.88	26.508	66.271
11	Block 11	12.2	9.4	12.68	2.19	23.17	25.032	62.581
12	Block 12	12.4	9.4	13.44	2.76	24.12	24.046	60.116
13	Block 13	12.6	9.4	11.83	2.18	21.48	27.002	67.505
14	Block 14	12.8	9.4	11.98	2.76	21.2	27.358	68.396
15	Block 15	11.6	9.6	11.34	2.65	20.03	28.957	72.391
16	Block 16	11.8	9.6	11.92	2.55	21.29	27.243	68.107
17	Block 17	12	9.6	12.91	2.49	23.33	24.861	62.152
18	Block 18	12.2	9.6	11.51	2.12	20.9	27.751	69.378
19	Block 19	12.4	9.6	11.49	2.03	20.95	27.685	69.212
20	Block 20	12.6	9.6	11.33	2.55	20.11	28.841	72.103
21	Block 21	12.8	9.6	12.86	2.48	23.24	24.957	62.392
22	Block 22	11.6	9.8	13.58	2.65	24.51	23.664	59.160
23	Block 23	11.8	9.8	11.48	2.42	20.54	28.238	70.594
24	Block 24	12	9.8	10.08	3.47	16.69	34.751	86.878
25	Block 25	12.2	9.8	13.02	2.57	23.47	24.712	61.781
26	Block 26	12.4	9.8	12.24	2.40	22.08	26.268	65.670
27	Block 27	12.6	9.8	10.58	2.94	18.22	31.833	79.583
28	Block 28	12.8	9.8	14.79	4.03	25.55	22.701	56.751
			Average	**12.01**	**2.62**	**21.39**	**27.598**	**68.996**

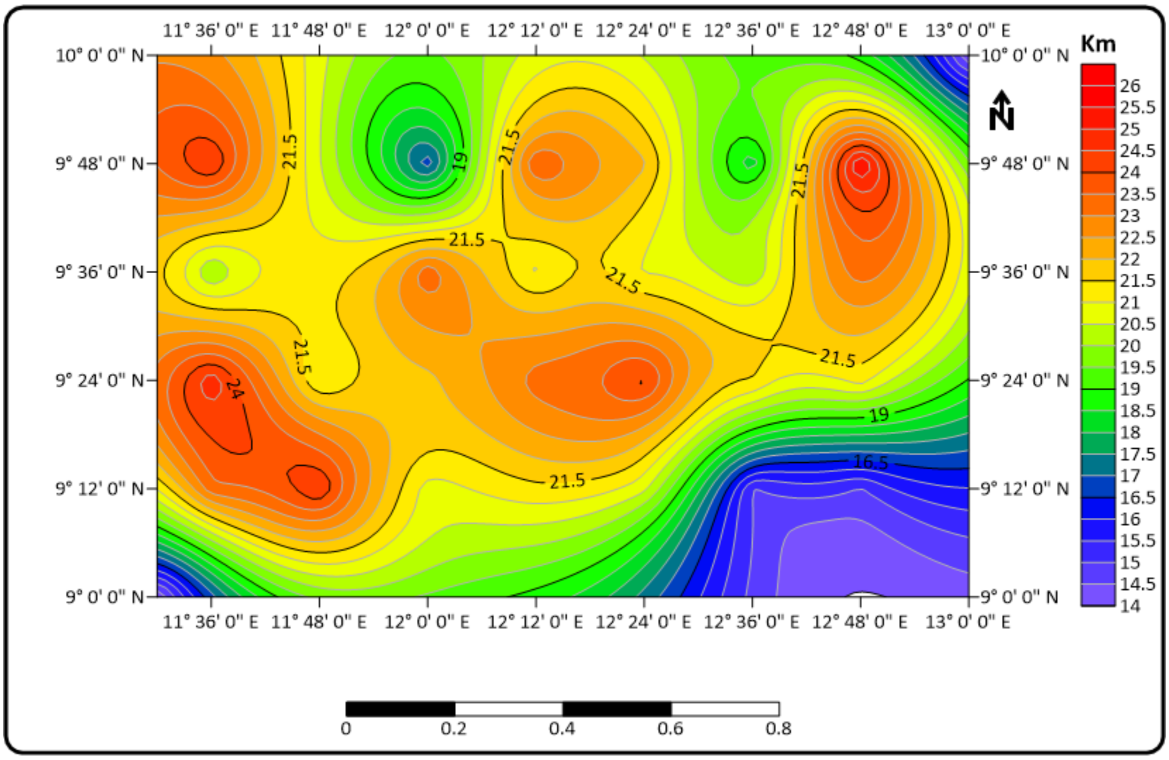

Figure 7: Contour map showing the study area's Curie point depth

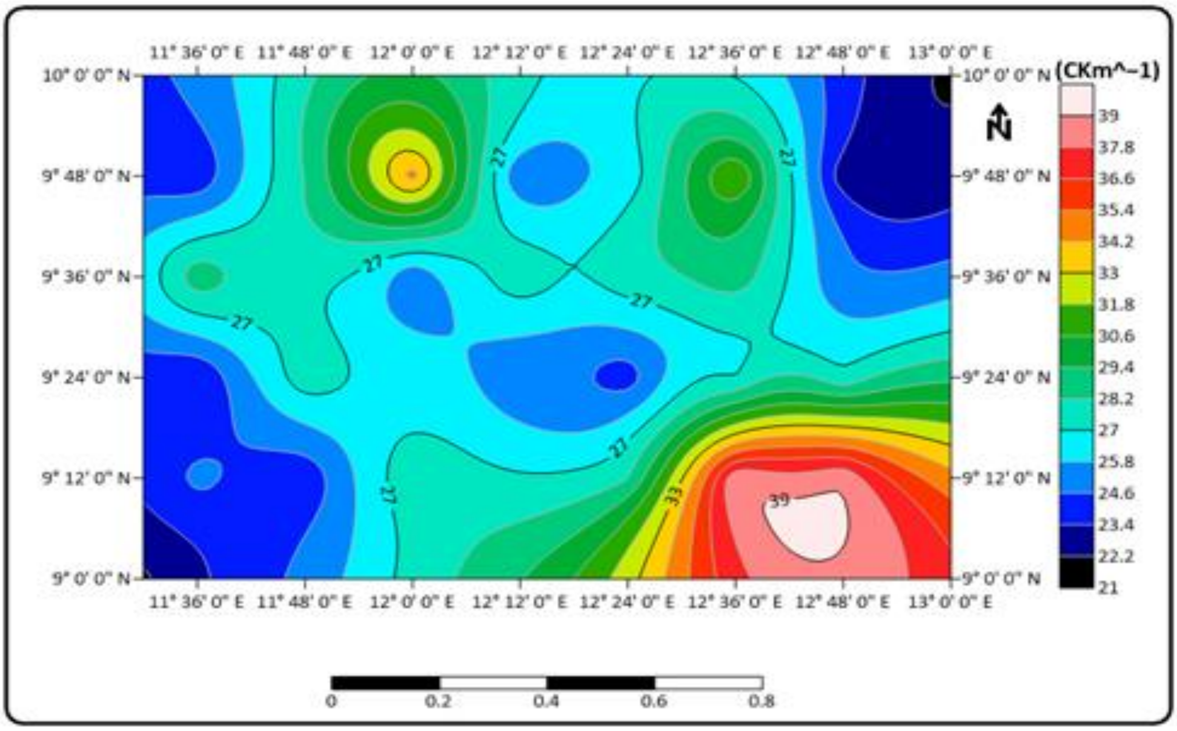

Figure 8: Contour map displaying the study area's geothermal gradient

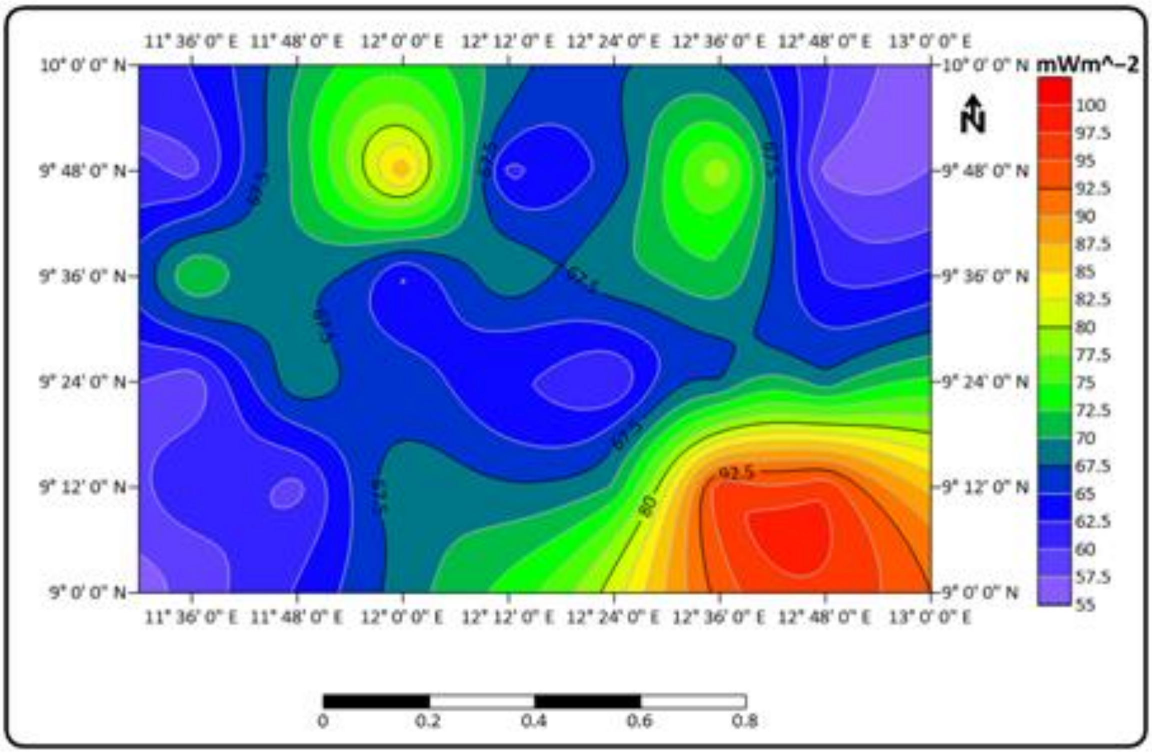

Figure 9: Contour map showing the study area's heat flow

The estimated geothermal gradients (22-39 °C/km) as seen in Fig. 8 are consistent with moderate to high thermal regimes typical of tectonically active regions(Turcotte & Schubert, 2002). Similarly, heat flow values ranging from 56 to 100 mW/m² (Fig. 9) with a mean value of about 69 mW/m² are relatively high compared to stable continental regions, where average values are typically below 60 mW/m² (Pollack *et al*., 1993). The observed inverse relationship between Curie depth and heat flow (Fig. 10) confirms that areas with shallow magnetic basement correspond to higher thermal activity (Tanaka *et al*., 1999).

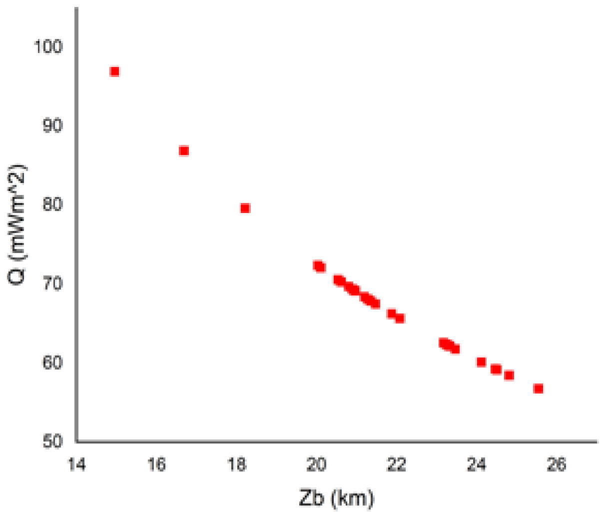

Figure 10: Relationship between heat Flow (Q) and Curie point depth (Z_b)

The southeast portion of the study area, marked by shallow CPD and high heat flow, is therefore interpreted as the most prospective zone for geothermal exploration. These findings are consistent with prior aeromagnetic studies conducted within Benue Trough (Abangwu *et al*., 2023; Kasidi & Nur, 2012; Nwankwo & Sunday, 2017; Odidi *et al*., 2020; Salako *et al*., 2019), thereby reinforcing the interpretation that the area possesses considerable potential for geothermal exploration and possible energy development.

CONCLUSION

The integration of spectral analysis with high-resolution aeromagnetic data has provided detailed insights into the subsurface thermal structure of the Yola Arm. Curie point depth (CPD) values vary between 14 km and 26 km, reflecting significant differences in crustal heat distribution. Shallower CPD zones (14–17 km) correspond to elevated geothermal gradients (22–39 °C/km) and higher heat flow (approximately 100 mW/m²), indicating moderate to high geothermal potential, while deeper CPD regions (>17 km) exhibit lower gradients and reduced heat flow, suggesting limited geothermal prospects (Tanaka *et al*., 1999; Turcotte & Schubert, 2002). Structural trends identified from the magnetic data are likely pathways for heat transfer, enhancing the feasibility of geothermal systems (Hochstein, 1990). Spatial analysis further highlights the southeast portion of the research area as the most favourable region for geothermal exploration due to the combination of shallow CPD, high heat flow, and thermally active structural features. These results demonstrate that the Yola Arm possesses considerable promise for geothermal resource development, particularly in structurally controlled zones that facilitate subsurface heat movement.

Conflict of interest: The authors declare no conflict of interest.

Acknowledgements: The authors appreciate the Tertiary Education Trust Fund (TETFund) for providing financial support through the Academic Staff Training and Development (AST&D) sponsorship programme. This support enabled access to funds necessary to successfully carry out this research.

REFERENCES

Abangwu, J. U., Okeke, F. N. and Obiora, D. N. (2023). Evaluation of geothermal energy potential of parts of Upper Benue Trough Nigeria using high resolution aeromagnetic data. *Indian Journal of Science and Technology*, 16(42), 3735–3742. https://doi.org/10.17485/IJST/v16i42.2201

Anakwuba, E. K. and Chinwuko, A. I. (2015). One dimensional spectral analysis and Curie depth isotherm of Eastern Chad Basin, Nigeria. *Journal of Natural Sciences Research*, 5(19), 14–22.

Anudu, G. K., Stephenson, R. A. and Macdonald, D. I. (2014). Using high-resolution aeromagnetic data to recognise and map intra-sedimentary volcanic rocks and geological structures across the Cretaceous middle Benue Trough, Nigeria. *Journal of African Earth Sciences*, 99, 625–636. https://doi.org/10.1016/j.jafrearsci.2014.02.017

Anudu, G. K., Stephenson, R. A., Ofoegbu, C. O. and Obrike, S. E. (2020). Basement morphology of the middle Benue Trough, Nigeria, revealed from analysis of high-resolution aeromagnetic data using grid-based operator methods. *Journal of African Earth Sciences*, 162, 103724. https://doi.org/10.1016/j.jafrearsci.2019.103724

Ayuba, M. G. and Lawal, M. K. (2019). Investigating geothermal energy resource potential in parts of South Western Nigeria using aeromagnetic data. *Science World Journal*, 14(3), 28–34.

Benkhelil, J. (1989). The origin and evolution of the Cretaceous Benue Trough (Nigeria). *Journal of African Earth Sciences*, 8(2–4), 251–282. https://doi.org/10.1016/S0899-5362(89)80028-4

Bhattacharyya, B. K. and Leu, L.-K. (1975). Analysis of magnetic anomalies over Yellowstone National Park: Mapping of Curie point isothermal surface for geothermal reconnaissance. *Journal of Geophysical Research*, 80(32), 4461–4465. https://doi.org/10.1029/JB080i032p04461

Blakely, R. J. (1996). *Potential Theory in Gravity and Magnetic Applications*. Cambridge University Press.

Carter, J. D. (1963). *The Geology of Parts of Adamawa, Bauchi and Borno Provinces in Northeastern Nigeria*. Geological Survey of Nigeria.

Dickson, M. H. and Fanelli, M. (2014). What is Geothermal Energy? *Istituto Di Geoscienze e Georisorse*. CNR, Pisa, Italy. Available at: http://mif.duo.netstrefa.pl/geothm_files/CO%20TO%20JEST%20GTH.pdf

DiPippo, R. and Renner, J. L. (2014). Geothermal energy. In: *Future energy* (pp. 471–492). Elsevier.

Hochstein, M. P. (1990). Classification and assessment of geothermal resources. In: *Small Geothermal Resources: A guide to Development and Utilization* (pp. 31–57). UNITAR.

International Renewable Energy Agency (2020). *Renewable Energy Statistics 2020*. Available at: https://www.irena.org/Publications/2020/Jul/Renewable-energy-statistics-2020

Kasidi, S. (2019). Determination of Curie point depth, heat flow and geothermal gradient from high resolution aeromagnetic data around Lamurde Area, Adamawa State, North-Eastern Nigeria. *Open Journal of Geology*, 9(11), 829–838. https://doi.org/10.4236/ojg.2019.911093

Kasidi, S. and Nur, A. (2012). Curie depth isotherm deduced from spectral analysis of magnetic data over Sarti and environs of North-Eastern Nigeria. *Scholarly Journal of Biotechnology*, 1, 49–56.

Minty, B. R. S. (1997). Fundamentals of airborne gamma-ray spectrometry. *AGSO Journal of Australian Geology and Geophysics*, 17, 39–50.

Nabighian, M. N., Grauch, V. J. S., Hansen, R. O., LaFehr, T. R., Li, Y., Peirce, J. W., Phillips, J. D. and Ruder, M. E. (2005). The historical development of the magnetic method in exploration. *Geophysics*, 70(6), 33ND–61ND. https://doi.org/10.1190/1.2133784

Nigerian Geological Survey Agency (2009). *Geological Map Sheets*. Available at: https://ngsa.gov.ng/geological-maps/

Nur, A., Ofoegbu, C. O. and Onuoha, K. M. (1999). Estimation of the depth of the Curie point isotherm in the Upper Benue Trough, Nigeria. *Journal of Mining and Geology*, 35.

Nwankwo, C. and Ekine, A. (2009). Geothermal gradients in the Chad Basin, Nigeria, from bottom hole temperature logs. *International Journal of Physical Sciences*, 4(12), 777–783.

Nwankwo, L. I. (2015). Spectral analysis of aeromagnetic data for geothermal investigation of Wikki warm spring, north-east Nigeria. *Geothermics*, 55, 207–208. https://doi.org/10.1016/j.geothermics.2014.05.016

Nwankwo, L. I. and Sunday, A. J. (2017). Regional estimation of Curie-point depths and succeeding geothermal parameters from high-resolution aeromagnetic data of the Bida Basin, Nigeria. *Geothermal Energy Science*, 5(1), 1–9. https://doi.org/10.5194/gtes-5-1-2017

Obaje, N. G. (2009). *Geology and Mineral Resources of Nigeria*. Springer.

Obande, G. E., Lawal, K. M. and Ahmed, L. A. (2014). Spectral analysis of aeromagnetic data for geothermal investigation of Wikki warm spring, north-east Nigeria. *Geothermics*, 50, 85–90. https://doi.org/10.1016/j.geothermics.2013.08.002

Odidi, I., Mallam, A. and Nasir, N. (2020). Investigation of geothermal energy potential using spectral analysis technique. *FUDMA Journal of Sciences*, 4(2), 627–638. https://doi.org/10.33003/fjs-2020-0402-248

Okubo, Y., Graf, R. J., Hansen, R. O., Ogawa, K. and Tsu, H. (1985). Curie point depths of Kyushu and surrounding areas, Japan. *Geophysics*, 50(3), 481–494. https://doi.org/10.1190/1.1441926

Oladunjoye, M. A., Olayinka, A. I., Alaba, M. and Adabanija, M. A. (2016). Interpretation of aeromagnetic data for lineament study in Ogbomoso area, Nigeria. *Journal of African Earth Sciences*, 114, 43–53. https://doi.org/10.1016/j.jafrearsci.2015.10.015

Patterson, N. R. and Reeves, C. V. (1985). Effects of the equatorial electrojet on aeromagnetic data acquisition. *Journal of Geophysics*, 55.

Pollack, H. N., Hurter, S. J. and Johnson, J. R. (1993). Heat flow from the Earth’s interior. *Reviews of Geophysics*, 31(3), 267–280. https://doi.org/10.1029/93RG01249

Rahaman, M. A. (1988). Recent advances in the study of the basement complex of Nigeria. In: *Pre-Cambrian Geology of Nigeria* (pp. 11–41). https://cir.nii.ac.jp/crid/1571135650759008768

Reeves, C. (2005). *Aeromagnetic Surveys: Principles, Practice and Interpretation*. Geosoft.

Spector, A. and Grant, F. S. (1970). Statistical models for interpreting aeromagnetic data. *Geophysics*, 35(2), 293–302. https://doi.org/10.1190/1.1440092

Tanaka, A., Okubo, Y. and Matsubayashi, O. (1999). Curie point depth based on spectrum analysis in East and Southeast Asia. *Tectonophysics*, 306(3–4), 461–470. https://doi.org/10.1016/S0040-1951(99)00072-4

Telford, W. M., Geldart, L. P. and Sheriff, R. E. (1990). *Applied Geophysics*. Cambridge University Press.

Turcotte, D. L. and Schubert, G. (2002). *Geodynamics*. Cambridge University Press.

Wright, J. B., Hastings, D. A., Jones, W. B. and Williams, H. R. (1985). *Geology and Mineral Resources of West Africa*. Springer.

Yakubu, J. A., Amuche, I. D., Igwe, A. E., Shuaibu, A. and Okwesili, A. N. (2023). Investigation of Curie point depth using aeromagnetic data in Lower Benue Trough Nigeria. *Indian Journal of Science and Technology*, 16(8), 540–546. https://doi.org/10.17485/IJST/v16i8.27

Zaborski, P., Ugodulunwa, F., Idornigie, A., Nnabo, P. and Ibe, K. (1997). Stratigraphy and structure of the Cretaceous Gongola Basin, northeast Nigeria. *Bulletin des Centres de Recherches Exploration-Production Elf-Aquitaine*, 21(1), 153–185.